Reliability Modelling of Power Electronics with Mission Profile Forecasting for Long-Term Planning

Sandelic, Monika; Sangwongwanich, Ariya; Peyghami, Saeed; Blaabjerg, Frede

Published in:
Proceedings of the 2022 IEEE 13th International Symposium on Power Electronics for Distributed Generation Systems (PEDG)

DOI (link to publication from Publisher):
10.1109/PEDG54999.2022.9923304

Publication date:
2022

Document Version
Accepted author manuscript, peer reviewed version

Reliability Modelling of Power Electronics with Mission Profile Forecasting for Long-Term Planning

Monika Sandelic, Ariya Sangwongwanich, Saeed Peyghami, Frede Blaabjerg
AAU Energy, Aalborg University, Aalborg DK-9220, Denmark
mon@energy.aau.dk, ars@energy.aau.dk, sap@energy.aau.dk, fbl@energy.aau.dk

***Abstract*—The power electronics system reliability is strongly dependent on the environmental and operating conditions at the installation site. During the reliability modelling, a mission profile-based procedure is traditionally employed to account for this dependency. To accurately estimate the reliability, mission profiles need to include the low resolution time intervals (e.g., several minutes per sample). The main forecasting challenge is the accurate prediction of such profiles for long-term prediction horizons, such as several years ahead. Therefore, in this paper, a mission profile forecasting method suitable for long-term reliability-oriented planning is proposed. The benefit of this method includes multi-year mission profile prediction with high time resolution (i.e., 1 minute per sample) suitable for power electronics reliability studies. A case study reveals that the proposed forecasting method enables power electronics modelling with less than 5% relative error in reliability estimation over different time horizons.**

***Index Terms*—Long-term forecasting, power electronics, reliability, design**

I. Introduction

Renewable energy-based systems, such as photovoltaic and wind power plants are nowadays designed for the operational span of 30-40 years [1]. The power converter design has a significant impact on the optimum design and reliable operation of such systems [2]. Data from the previous field experience indicate power electronics failure as the one of the leading reasons for system downtime [3]. For example, power electronics failure was listed as one of the top five common failure causes of wind power plants in UK [4]. Moreover, in the photovoltaic applications, it is reported that the half of the system failures were attributed to the power electronics [5]. Similar is concluded in [6], where it is shown that the power converter reliability design significantly impacts the maintenance strategies and long-term system planning. Therefore, design for reliability of power converters needs to be included in the process of the system design.

The power electronics reliability is strongly dependent on the application-specific operating and environmental conditions. Those conditions are included in the form of a mission profile for which the power converter reliability is determined during the design process. If the reliability level is not sufficient, corrective design actions are performed until an optimum design is reached [7]. To assure accurate prediction of the converter reliability, several requirements are set for the mission profile. 1) Mission profile needs to accurately represent the operating conditions at the installation site [8]. 2) The time horizon of the mission profile needs to match the design horizon of the system the power converter is a part of [9]. 3) The time resolution needs be in a minute range to capture the changes in the converter loading that cause damage accumulation [10].

A common way to represent the operating conditions is to use historical data of the installation site as a mission profile [11]. For example, in solar photovoltaic applications, one year historical data are used to represent expected intra-year and seasonal patterns [12]. It is assumed that the estimated yearly degradation occurs repetitively until the failure of the unit due to wear-out happens [13]. In such approach, inaccuracies are introduced due to using historical data instead of predicted data, as well as using only a single year instead of several years. The later is investigated in [14], [15]. In [14], it is reported that using a one-year mission profile repetitively instead of five years of historical data introduces 7% error in the reliability estimation. However, the analysis was conducted for a installation site in an arid climate, which impacted the accuracy of the results to large extend. In [15], the mission profiles with a higher level of intra-year variations are examined. The difference in failure percentage of more than 20% is reported. In fact, the study concluded that a single-year mission profile approach can lead to significant differences in the optimum design solution. Further on, it can be assumed that the error becomes more pronounced for longer design horizons. Another approach includes simplifications of the mission profile. For example, in [16], a mission profile is generated based on the application-specific operating scenario with the highest probability of occurrence. However, the impact of the assumptions on the accuracy of the reliability prediction in the long-term planning is not investigated.

A more accurate approach would be to use a forecasting method to predict the mission profile instead of using historical data. The long-term planning methods used in power system domain can be used to predict environmental conditions for several decades ahead [17]. Hence, those methods match the mission profile time horizon requirement. However, in the power system domain, the forecast profiles require significantly lower time resolution (e.g., 1 month or 1 year per sample) than the ones for power electronics reliability applications. To overcome this issue, the short-term forecasting method can be used to generate the high resolution profiles [18]. Nonetheless, their accuracy decreases as time horizons extends [19]. Therefore, they are not suitable for time horizons in a range of years.

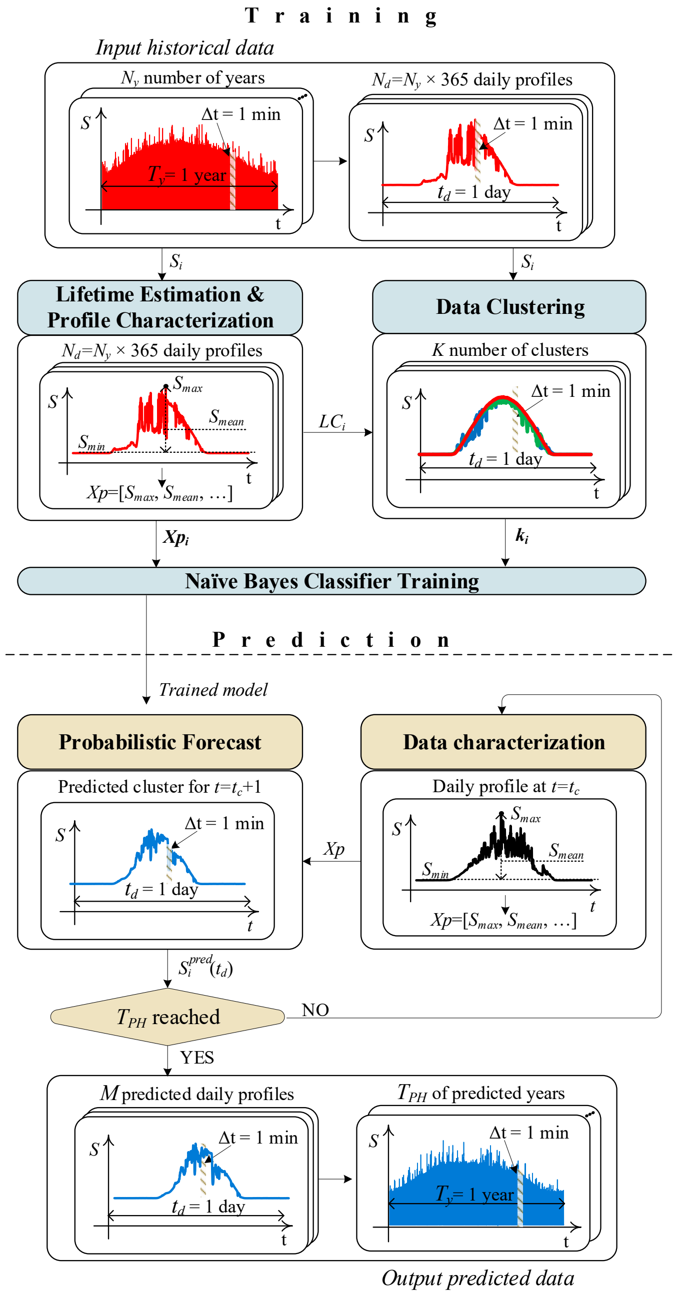

Fig. 1. Proposed mission profile forecasting framework for reliability modelling of power converters in the long-term planning shown on the example of solar irradiance S. Input is N_y years of historical data with $\Delta t = 1$ min/sample resolution, output is T_{PH} years of predicted data with $\Delta t = 1$ min/sample resolution.

In this paper, an approach to do long-term mission profile forecasting for reliability modelling of power converters is presented. The proposed approach connects the long-term forecasting methods with the time resolution requirements of the power converters reliability modelling. Hence, it overcomes the limitations of long-term forecasting methods in application to mission profile prediction for power electronics reliability studies. The rest of the paper is organized as follows.

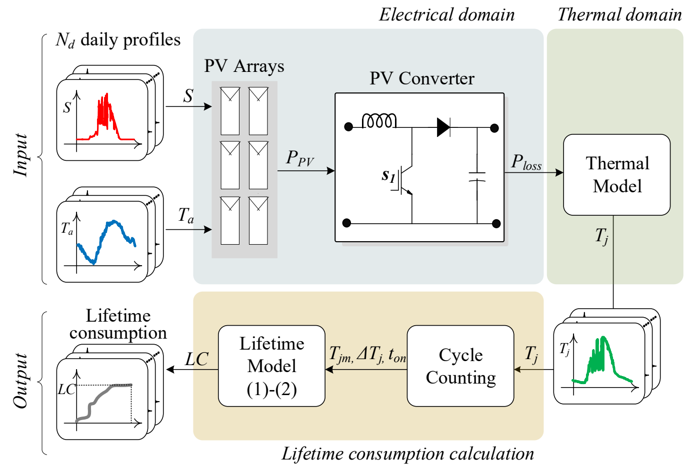

Fig. 2. Procedure for determination of the lifetime consumption LC for input solar irradiance S and ambient temperature T_a profiles on the example of the photovolatic (PV) arrays connected to the DC/DC boost converter. P_{PV} is output power of PV arrays, P_{loss} is DC/DC converter loss, T_j is junction temperature of Insulated-Gate Bipolar Transistor s_1, T_{jm} and ΔT_j are mean and cycle amplitude of the junction temperature, and t_{on} is a cycle period.

In Section II, a detailed description of the framework for mission profile forecasting is provided. In Section III, a case study is conducted, where the forecast accuracy for reliability modelling is examined. In Section IV, the main conclusions of the study are provided.

II. The Proposed Framework

The proposed framework for mission profile forecasting in design for reliability of power converters is shown in Fig. 1. It can be used for a multi-year forecasting with a high time resolution (e.g., 1 minute per sample), which is suitable for reliability modelling of power electronics. The framework consists of two main parts, namely training and prediction.

As part of the training process, historical data is organized into daily profiles. These profiles are then characterized and clustered into characteristic daily profiles. Afterwards, the Naïve Bayes Classifier is used to determine the conditional probability of each characteristic daily profile occurrence given daily characteristics. In the second step, a daily profile is characterized and used together with the trained model for prediction. More details on the implementation of each step are provided in following.

A. Training Process

The input to the training process are N_y profiles of historical data. Each profile has a time horizon T_y of one year and a time resolution Δt of 1 minute per sample. The N_y profiles are sorted into $N_d = N_y \times 365$ daily profiles (time horizon $t_d = 1$ day). During the training process, the daily profiles are divided into clusters based on their impact on power electronics reliability.

1) Lifetime Estimation & Profile Characterization: A lifetime consumption LC is selected as a relevant reliability parameter. Its value is determined for each daily profile in the input training set by following the procedure shown in Fig. 2. To determine LC, a converter loading for the input conditions (i.e., daily mission profile) is first investigated. Then, the junction temperature T_j of the Insulated-Gate Bipolar Transistor (IGBT), being the reliability-critical component considered in this paper, is determined by means of an electro-thermal model [20]. The relevant stress information, such as mean junction temperature T_{jm}, the cycle amplitude ΔT_j and the cycle period t_{on}, are extracted from T_j profile. Those are used to determine the number of cycles to failure N_f described with the lifetime model in (1) based on [21]. Then, LC is defined in (2) as a ratio of the number of cycles for given operating conditions n_i and the number of cycles to failure N_f.

$$\begin{aligned} N_f = \; & K \cdot (\Delta T_j)^{\beta_1} \cdot e^{\frac{\beta_2}{T_{jm}+273}} \cdot \\ & (t_{on})^{\beta_3} \cdot I^{\beta_4} \cdot V^{\beta_5} \cdot D^{\beta_6} \end{aligned} \tag{1}$$

$$LC = \sum_i \frac{n_i}{N_{fi}} \tag{2}$$

Each daily profile is also characterized by series of features and included in the feature array X_p. The features are defined with respect to the parameters, which best describe the characteristic of the daily profiles and can provide information about the daily, weekly and monthly characteristics. For example, those parameters can be daily mean, peak, standard deviation, and maximum difference between two samples in the profile.

2) Data Clustering: The K-means method discussed in [22] is used to optimally cluster the LC values of each daily profile. The method is used to find the optimal number of clusters, where all the LC values belonging to one cluster have the highest degree of associations and vice versa. The objective function to be minimized is defined as follows:

$$J = \sum_{i=1}^{N_d} \sum_{k=1}^{K} u_{ik} \| LC_i - C_k \| \tag{3}$$

where C_k is k-th cluster centroid and u_{ik} represent the membership of the i-th LC to a cluster k.

Therefore, the output of the clustering process is K number of clusters, where the k-th cluster is represented with a cluster centroid C_k. This value is a mean value of all the LC values belonging to the cluster. To find the characteristic daily profiles, cluster centroid C_k is compared to all LC elements belonging to the cluster k. Daily profiles of the element with LC closest to C_k are used to represent the characteristic profiles of a cluster.

3) Naïve Bayes Classifier Training: In this step, the probability of the occurrence of a cluster k given certain conditions in X_p needs to be determined. This is done by means of Naïve Bayes Classifier [23]. Input to the model is a matrix which consists of the feature array X_p and cluster information for each daily profile in the training set. Hence, during training, both features and association to certain cluster are known for each day in the input training set. Therefore, Naïve Bayes Classifier determines the prior probability distribution for each cluster with respect to input matrix information. Moreover, it evaluates the probability of features given that the outcome cluster is know (i.e., likelihood). The output of the procedure is the trained model, which is then used in the prediction process.

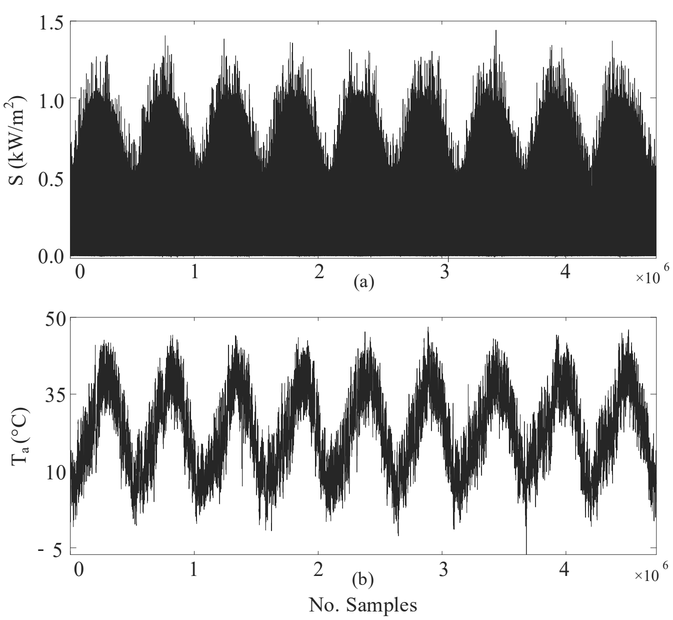

Fig. 3. Training data set (9 years) with 1 minute per sample time resolution for Las Vegas, Nevada installation site: (a) Solar irradiance S, and (b) Ambient temperature T_a.

B. Prediction Process

A probabilistic forecast is employed to determine a multi-year mission profile, which is a combination of the characteristic daily profiles. The input to the prediction is X_p array, that is defined based on the characteristics of the previously

TABLE I
CASE STUDY: SYSTEM DESIGN PARAMETERS AND CHARACTERISTICS.

PV array rated power	7.2 kW
DC/DC converter rated power	6 kW (3kW x 2 units)
Reliability-critical component	IGBT (s_1)
Failure mechanism	Bond wire lift-off
Stress parameter	Junction temperature T_j of s_1
Lifetime model	Number of cycles to failure N_f

TABLE II
CASE STUDY: IGBT LIFETIME MODEL PARAMETERS.

Factor	Value	Description	Constant	Value
			β_1	-4.416
I	10 A	Bond wire current	β_2	1285
V	0.6 kV	Blocking voltage	β_3	-0.463
D	300 μm	Bond wire diameter	β_4	-0.716
K	2.03×10^{14}	Technology factor	β_5	-0.761
			β_6	-0.5

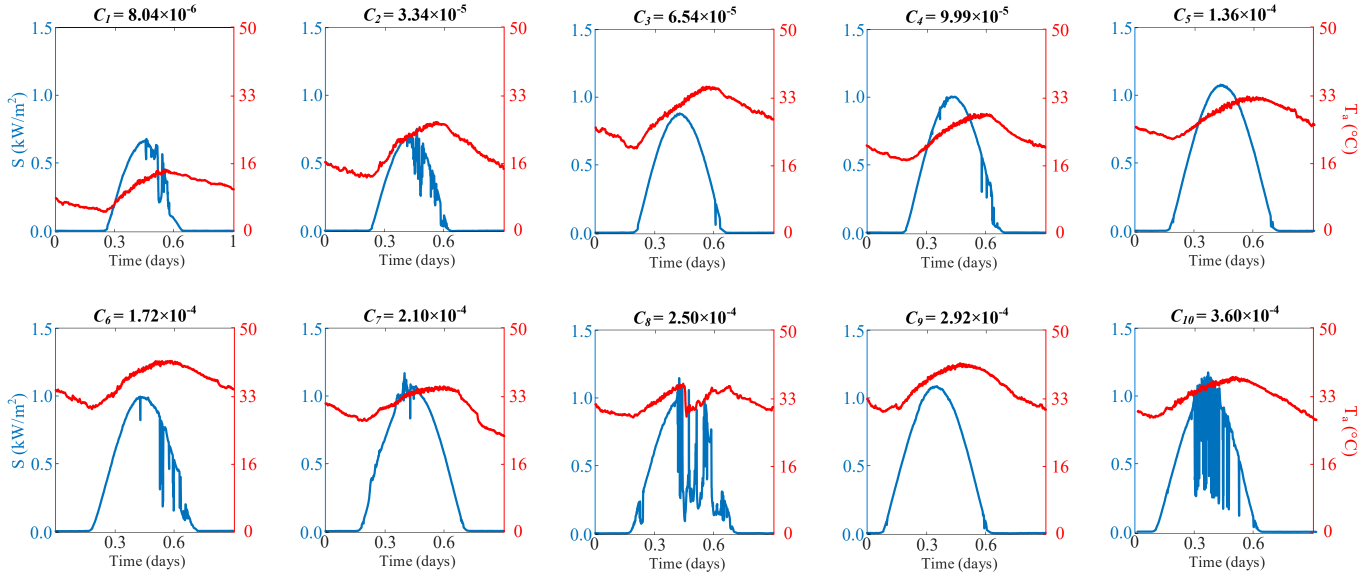

Fig. 4. Clustering results for input training set (9 years of data with 1 minute per sample resolution) yielding $K = 10$ clusters ($C_1 - C_{10}$). Each cluster is characterized by the cluster centroid C_k and characteristic daily profiles (1 minute per sample resolution) of solar irradiance S (blue curve) and ambient temperature T_a (red curve).

determined daily profiles. The process of defining X_p is the same as in the case of model training. However, the data used to define X_p are observation and prediction data, which differ from the training data. Information in X_p are used together with the trained model based on the Naïve Bayes Classifier to find the cluster with the highest probability of occurrence for the following day, which is defined as [23]:

$$\begin{aligned} &max(P(S_i^{pred} = C_k|X_p)) = \\ &max\left\{\prod_{l=1}^{L} P(X_{p_i}(l)|S_i^{pred} = C_k) \cdot P(S_i^{pred} = C_k)\right\} \end{aligned} \tag{4}$$

where S_i^{pred} is the i-th daily predicted profile, $X_{p_i}(l)$ is the l-th feature of the i-th day feature array, and L is the length of the feature array.

Once a daily profile is predicted, it is used as the input to the procedure to predict the subsequent profile. The process is repeated until the prediction horizon T_{PH} is reached.

III. Case Study

A. Case Study Description

The proposed framework is demonstrated on an example of the photovoltaic arrays connected to the DC/DC converter (see Fig. 2). The main characteristics of the system are provided in Table I. Moreover, the lifetime data for the switch s_1 used in the lifetime model described by (1) is given in Table II.

The input to the PV array is solar irradiance S and ambient temperature T_a, which need to be predicted. In the first step, the forecast model is trained on the input training data set shown in Fig. 3. Training data consists of $N_d = 3285$ daily profiles ($N_y = 9$ years $\times$ 365 days). They corresponds to the historical data for installation site in Las Vegas, Nevada in period from 2008 to 2016 [24]. In the second step, the trained model is used to predict solar irradiance S^{pred} and ambient temperature T_a^{pred} profiles for $T_{PH} = 4$ years (2017-2020).

B. Mission Profile Forecasting

Training results are shown in Fig. 4, where the output of the cluster procedure is shown. The input training set ($N_d =$ 3285 daily profiles) is clustered into $K = 10$ characteristic clusters. The optimum number of clusters is determined by Calinski-Harabasz criterion [25]. Each cluster is represented with centroid C_k (i.e., mean LC value) and the characteristic daily S and T_a profiles. The centroid results show that the higher LC values are represented with more clusters than the low LC values. This refers to that a larger number of daily profiles belong to e.g., the cluster with centroid C_1 than the cluster with centroid C_{10}. In the case of low LC values, a similar result is obtained, regardless of differences in low S and T_a daily profiles. Therefore, more profiles are clustered together. In contrary to this, high daily S and T_a contribute more to the LC accumulation. The differences in those daily profiles lead to a larger variation of LC. Thus, a larger number of clusters need to be defined to assure that reliability can be determined accurately based on the forecast mission profiles.

The obtained characteristic profiles are used in the prediction process to construct the forecast profiles of solar irradiance S^{pred} and ambient temperature T_a^{pred} by using trained Naïve Bayes Classifier. The forecast results are shown in Fig. 5 together with the actual data (historical profiles for 2016-2020). There are certain discrepancies between predicted and actual profiles, which need to be investigated. However, the traditional metrics for evaluation of forecast accuracy, such as mean average error, are not suitable in this case. Those

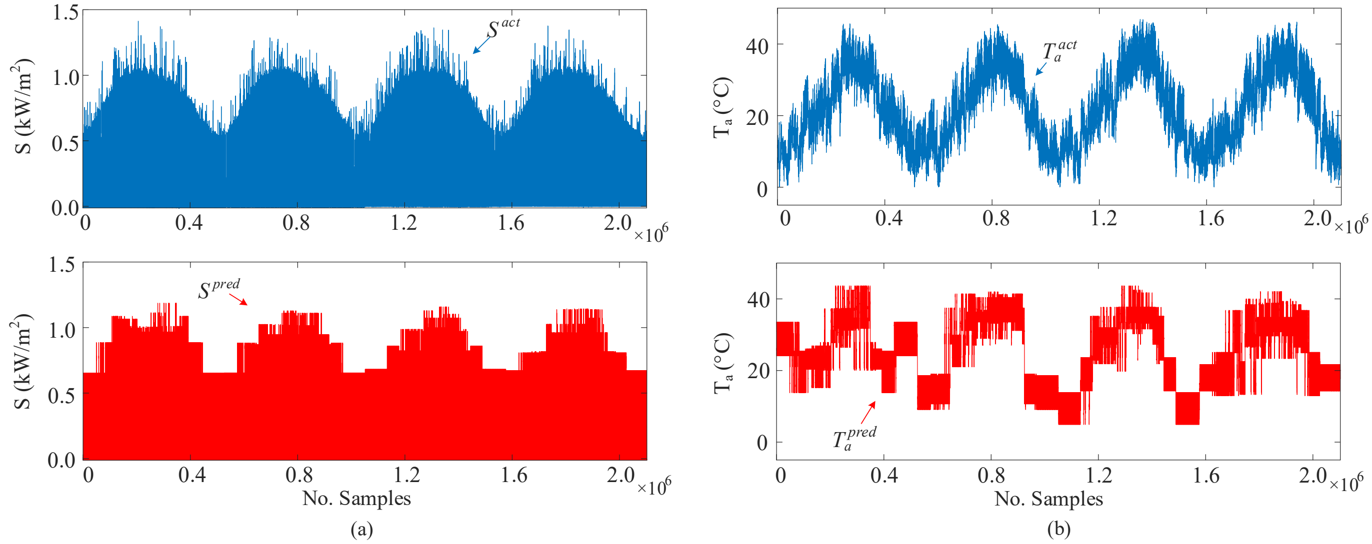

Fig. 5. 4-year profiles of solar irradiance S and ambient temperature T_a with 1 minute per sample resolution: (a) Actual profiles, and (b) Predicted profiles which are a combination of the $K = 10$ daily cluster profiles with probability of occurence determined with Naïve Bayes Classifier .

metrics investigate point difference between actual and predicted profiles. Such approach does not align with the forecast accuracy requirements in this study. The predicted profiles are used as mission profiles to determine the reliability of the power converter. Therefore, the suitability of the predicted profiles accuracy for usage in design for reliability of power electronics needs to be evaluated, as done in following.

C. Forecasting Accuracy for Reliability Modelling

To investigate the accuracy of the predicted profiles for reliability studies, three cases are studied. In each case, a different input mission profile is used to evaluate LC of DC/DC converter. In the first case, the actual solar irradiance S^{act} and ambient temperature T_a^{act} profiles for period 2017-2020 are used. This case includes profiles with 100% forecast accuracy, and the output result is marked as LC^{act}. In the second case, the predicted profiles S^{pred} and T_a^{pred} that are obtained with the proposed model are used. The purpose of this case is to investigate the impact of forecast inaccuracy on reliability results. The output result is marked as LC^{pred}. In the third case, a one-year historical profile from 2016 (last year of training data in Fig. 3) is repetitively used for four years. This case represents a state-of-art approach to design for reliability. The output result is marked as LC^{hist}.

Yearly LC results for the three cases are shown in Fig. 6(a). LC^{pred} is closer to LC^{act} than LC^{hist} in each year. This shows that using predicted results for each year is a more favorable option than repetitively using one-year historical data. To investigate further the impact of predicted and historical mission profile on the reliability accuracy, the

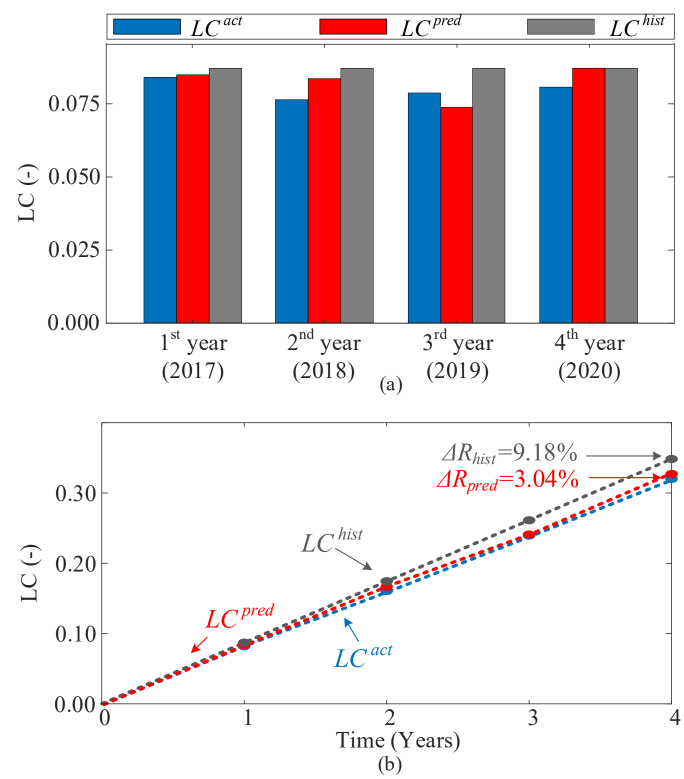

Fig. 6. Lifetime consumption results for three different input profiles: (a) Each individual year, and (b) Accumulated over 4 years.

following metrics is applied:

$$\Delta R_{pred} = \left| \frac{LC^{pred} - LC^{act}}{LC^{act}} \right| \times 100\% \tag{5}$$

$$\Delta R_{hist} = \left| \frac{LC^{hist} - LC^{act}}{LC^{act}} \right| \times 100\% \tag{6}$$

TABLE III
CASE STUDY RESULTS: LIFETIME CONSUMPTION ACCURACY FOR PREDICTED AND HISTORICAL MISSION PROFILES.

No. years	1 year (2017)	2 years (2017-2018)	3 years (2017-2019)	4 years (2017-2020)
ΔR_{pred}	1.19%	5.06%	1.30%	3.04%
ΔR_{hist}	3.94%	8.81%	9.47%	9.18%

where ΔR_{pred} is a relative error between yearly LC^{pred} and LC^{act}, while ΔR_{hist} is a relative error between yearly LC^{hist} and LC^{act}.

The accumulated LC results are shown in Fig. 6(b). Moreover, the relative errors ΔR_{pred} and ΔR_{hist} are summarized in Table III. The predicted mission profiles, even though represented with only 10 characteristic daily profiles, results in a reliability prediction error significantly lower than the one of the historical mission profiles. In fact, the difference in the relative error of the two cases is becoming larger as the time horizon extends. Therefore, it is more accurate to use predicted results than repetitively use one-year historical data. Furthermore, ΔR_{pred} reveals that the predicted mission profile results with no more than approximately 5% error regardless the time horizon investigated. Therefore, the predicted mission profile can be used in the reliability modelling of power electronics.

IV. CONCLUSION

In this paper, a mission profile forecasting framework for reliability modelling of power converters is presented. The proposed framework considers power electronics reliability within the forecasting procedure. Case study results indicate that the forecast mission profile can be used for the reliability modelling of power converters. In fact, the reliability prediction results indicate that the relative error in yearly lifetime consumption of the predicted mission profile is less than 5% over a four year prediction range.

ACKNOWLEDGMENT

This work was supported by the Reliable Power Electronic-Based Power System (REPEPS) project at the AAU Energy, Aalborg University as part of the Villum Investigator Program funded by the Villum Foundation.

REFERENCES

[1] International Renewable Energy Agency (IRENA), "Future of solar photovoltaic: Deployment, investment, technology, grid integration and socio-economic aspects (a global energy transformation paper)," Abu Dahbi, 2019.

[2] H. Wang and F. Blaabjerg, "Power electronics reliability: State of the art and outlook," *IEEE J. Emerg. Sel. Top. Power Electron.*, vol. 9, no. 6, pp. 6476–6493, 2021.

[3] S. Yang, A. Bryant, P. Mawby, D. Xiang, L. Ran, and P. Tavner, "An industry-based survey of reliability in power electronic converters," in *Proc. of ECCE*, San Jose, CA, USA, 2009, pp. 3151–3157.

[4] System Performance, Availability and Reliability Trend Analysis SPARTA, "Portfolio review 2016," , 2020. [Online]. Available: https://www.sparta-offshore.com. Accessed: Jun. 21, 2021.

[5] Kiwa, "Addressing the challenges of string inverter failures in solar PV systems," 2021. [Online]. Available: https://www.kiwa.com/nl/en/. Accessed: Jan. 5, 2022.

[6] S. Peyghami, F. Blaabjerg, J. R. Torres, and P. Palensky, "Maintenance scheduling in power electronic converters considering wear-out failures," in *Proc. of EPE'20 ECCE Europe*, Lyon, France, 2020, pp. 1–10.

[7] M. Musallam, C. Yin, C. Bailey, and M. Johnson, "Mission profile-based reliability design and real-time life consumption estimation in power electronics," *IEEE Trans. Power Electron.*, vol. 30, no. 5, pp. 2601–2613, 2015.

[8] V. de Nazareth Ferreira, A. Fagner Cupertino, H. Augusto Pereira, A. Vagner Rocha, S. Isaac Seleme, and B. de Jesus Cardoso Filho, "Design and selection of high reliability converters for mission critical industrial applications: A rolling mill case study," *IEEE Trans. Ind. Appl.*, vol. 54, no. 5, pp. 4938–4947, 2018.

[9] M. Sandelic, S. Peyghami, A. Sangwongwanich, and F. Blaabjerg, "Reliability aspects in microgrid design and planning: Status and power electronics-induced challenges," *Renew. Sust. Energ. Rev.*, vol. 159, pp. 112 127–112 144, 2022.

[10] A. Sangwongwanich, D. Zhou, E. Liivik, and F. Blaabjerg, "Mission profile resolution impacts on the thermal stress and reliability of power devices in PV inverters," *Microelectron. Reliab.*, vol. 88-90, pp. 1003–1007, 2018.

[11] Y. Yang, A. Sangwongwanich, and F. Blaabjerg, "Design for reliability of power electronics for grid-connected photovoltaic systems," *CPSS Trans. Power Electron. Appl.*, vol. 1, no. 1, pp. 92–103, 2016.

[12] R. Silva, R. de Barros, E. Brito, W. Boaventura, A. Cupertino, and H. Pereira, "Pursuing computationally efficient wear-out prediction of PV inverters: The role of the mission profile resolution," *Microelectron. Reliab.*, vol. 110, pp. 113 679–113 687, 2020.

[13] L. Gusman, H. Pereira, J. Callegari, and A. Cupertino, "Design for reliability of multifunctional PV inverters used in industrial power factor regulation," *Int. J. Electr. Power Energy Syst.*, vol. 119, pp. 105 932–105 941, 2020.

[14] A. F. Cupertino, J. M. Lenz, E. M. Brito, H. A. Pereira, J. R. Pinheiro, and S. I. Seleme, "Impact of the mission profile length on lifetime prediction of PV inverters," *Microelectron. Reliab.*, vol. 100, pp. 113 427–113 432, 2019.

[15] M. V. Kjaer, Y. Yang, H. Wang, and F. Blaabjerg, "Long-term climate impact on IGBT lifetime," in *Proc. of EPE'20 ECCE Europe*, Lyon, France, 2020, pp. 1–10.

[16] J. Harikumaran, G. Buticchi, G. Migliazza, V. Madonna, P. Giangrande, A. Costabeber, P. Wheeler, and M. Galea, "Failure modes and reliability oriented system design for aerospace power electronic converters," *IEEE Open J. Ind. Electron. Soc.*, vol. 2, pp. 53–64, 2021.

[17] Z. Ding, X. Wen, Q. Tan, T. Yang, G. Fang, X. Lei, Y. Zhang, and H. Wang, "A forecast-driven decision-making model for long-term operation of a hydro-wind-photovoltaic hybrid system," *Appl. Energy*, vol. 291, p. 116820, 2021.

[18] L. Jiang, X. Wang, W. Li, L. Wang, X. Yin, and L. Jia, "Hybrid multitask multi-information fusion deep learning for household short-term load forecasting," *IEEE Trans. Smart Grid*, vol. 12, no. 6, pp. 5362–5372, 2021.

[19] A. Ahmed and M. Khalid, "A review on the selected applications of forecasting models in renewable power systems," *Renew. Sust. Energ. Rev.*, vol. 100, pp. 9–21, 2019.

[20] A. Sangwongwanich, Y. Yang, D. Sera, and F. Blaabjerg, "Mission profile-oriented control for reliability and lifetime of photovoltaic inverters," *IEEE Trans. Ind. Appl.*, vol. 56, no. 1, pp. 601–610, 2020.

[21] R. Bayerer, T. Herrmann, T. Licht, J. Lutz, and M. Feller, "Model for power cycling lifetime of IGBT modules - various factors influencing lifetime," in *Proc. of CIPS*, Nuremberg, Germany, 2008, pp. 1–6.

[22] K. P. Sinaga and M.-S. Yang, "Unsupervised k-means clustering algorithm," *IEEE Access*, vol. 8, pp. 80 716–80 727, 2020.

[23] Y. Yang, W. Li, T. A. Gulliver, and S. Li, "Bayesian deep learning-based probabilistic load forecasting in smart grids," *IEEE Trans. Industr. Inform.*, vol. 16, no. 7, pp. 4703–4713, 2020.

[24] T. Stoffel, and A. Andreas, National Renewable Energy Laboratory (NREL), "University of Nevada (UNLV): Las Vegas, Nevada (Data)," Tech. Rep. No. DA-5500-56509, 2006.

[25] U. Maulik and S. Bandyopadhyay, "Performance evaluation of some clustering algorithms and validity indices," *EEE Trans. Pattern Anal. Mach. Intell.*, vol. 24, no. 12, pp. 1650–1654, 2002.